HOSTED BY

ELSEVIER

Available online at www.sciencedirect.com

ScienceDirect

Journal of Computational Design and Engineering 3 (2016) 312–321

www.elsevier.com/locate/jcde

Dynamic analysis and controller design for a slider–crank mechanism with piezoelectric actuators

Samin Akbari[a,*], Fatemeh Fallahi[b], Tohid Pirbodaghi[a]

[a]*Mechanical Engineering Department, Massachusetts Institute of Technology, 77 Massachusetts Avenue, Cambridge, MA, USA*
[b]*University of Alberta, Edmonton, Canada*

Received 9 March 2016; received in revised form 20 May 2016; accepted 23 May 2016
Available online 3 June 2016

Abstract

Dynamic behaviour of a slider–crank mechanism associated with a smart flexible connecting rod is investigated. Effect of various mechanisms' parameters including crank length, flexibility of the connecting rod and the slider's mass on the dynamic behaviour is studied. Two control schemes are proposed for elastodynamic vibration suppression of the flexible connecting rod and also obtaining a constant angular velocity for the crank. The first scheme is based on feedback linearization approach and the second one is based on a sliding mode controller. The input signals are applied by an electric motor located at the crank ground joint, and two layers of piezoelectric film bonded to the top and bottom surfaces of the connecting rod. Both of the controllers successfully suppress the vibrations of the elastic linkage.

Keywords: Slider–crank mechanism; Flexible connecting rod; Piezoelectric; Dynamic response, Nonlinear controller

1. Introduction

High operating speed, superior reliability and accurate performance are major characteristics of modern industrial machinery and commercial equipments. A traditional rigid-body analysis, which presumes low operating speeds, becomes insufficient to describe the performance of such high speed systems. A thorough understanding of the dynamic behaviour of the modern machines undergoing high-speed operations, which are based on multibody systems such as slider–crank mechanisms, is necessary. Several researchers have worked on development of suitable formulations with these mechanisms. Neubauer et al. examined the transverse deflection of an elastic connecting rod of a slider–crank mechanism by neglecting the longitudinal deformation, the Coriolois, relative tangential and relative normal components of the acceleration [1]. Hsieh and Shaw studied the nonlinear resonance of a flexible connecting rod by considering both longitudinal and transverse deflection of the rod [2]. They investigated that the connecting rod behaves as a system with a softening type of nonlinearity, which is subjected to external and parametric excitations. Chen and Chian studied effect of crank length on the dynamic behaviour of damped flexible connecting rod [3]. Zheng et al. and Muvengi et al. have considered the effect of joint clearance and Reis et al added the effect of friction in dynamic analysis of the mechanism [4–6]. Complexity of the dynamic model of flexible mechanisms and their high nonlinearities make these systems hard to control. A few researchers have attempted to reduce or eliminate the vibrations of flexible mechanisms induced by one or more of the flexible links [7–9].

Karkoub and Yigit designed a controller for a four-bar mechanism with a flexible coupler. Their closed-loop system was able to trace a prescribed motion at the input link level. The PD controller was able to move the mechanism to the desired position and absorb the elastodynamic vibrations [10]. Karkoub has also developed a controller based on μ synthesis for suppressing the elastodynamic vibrations of a slider–crank mechanism associated with a very flexible connecting rod [11]. Sannah and Smaili designed a multivariable optimal controller for a four-bar mechanism with a flexible coupler using a finite

*Corresponding author. Tel.: +1 617 810 9643; fax: +1 617 810 9642.
E-mail address: sakbari@mit.edu (S. Akbari).
Peer review under responsibility of Society of CAD/CAM Engineers.

http://dx.doi.org/10.1016/j.jcde.2016.05.002

Nomenclature

r	crank length
L	connecting rod length
θ	crank angle
ψ	connecting rod angle with respect to the ground
$q_i(t)$	modes of vibrations of the flexible slider–crank mechanism
F_i	nonconservative forces
τ_i	applied torque on the system
$\vec{\xi}$	deflection vector
Ic	moment of inertia of the crank
A	cross section of the connecting rod
Ms	slider mass
Mc	crank mass
EI	flexural rigidity
ρ	material density
H	radius of the rod
d_{31}	dielectric coefficient
V	applied voltage to piezoelement
$\vec{X}_B$	velocity of the connecting rod end point

element dynamics model. The results were implemented on an experimental test bed using a pair of piezoceramic sensors/actuators [12].

Here, we focus on studying effect of various mechanisms' parameters on the dynamic behaviour and rotation of the crank considering the transverse deflection of the connecting rod. Even with no external excitation, rotation of the crank excites the connecting rod and induces vibration. We successfully suppressed the vibrations of the elastic linkage using two piezoelectric actuators and nonlinear controllers designed based on feedback linearization and sliding mode.

2. Modeling of the mechanism

Equation of motion of a flexible slider–crank mechanism is derived using the Euler–Lagrange approach [13–17]. The mechanism is assumed to move in the horizontal plane and the longitudinal defections are negligible. Schematic of the slider–crank mechanism with a flexible connecting rod is depicted in Fig. 1. The mechanism parameters are defined as follows: r is the crank length; L is the connecting rod length; θ is the crank angle; $\psi$is the connecting rod angle with respect to the ground; x and w are the x- and y-coordinates, respectively, of any point on the connecting rod in the $\vec{e}_1 - \vec{e}_2$ coordinate system.

The location of any point on the flexible connecting rod (Fig. 1) is given by

$$\vec{R} = \vec{r} + \vec{x} + \vec{w} \tag{1}$$

equal to

$$\vec{R} = (r\cos\theta + w\cos\psi + x\cos\psi)\,\vec{i} + (r\sin\theta + w\sin\psi - x\sin\psi)\,\vec{j} \tag{2}$$

The y-component of the displacement of the end point of the connecting rod at $x=l$, which can be obtained by taking the scalar product of the displacement vector $\vec{R}$ and $\vec{j}$ is equal to zero. Therefore

$$\psi = \sin^{-1}\left(\frac{r}{l}\sin\theta\right) \tag{3}$$

Using the mode summation technique, the deflection w is given by

$$w = \sum_{i=1}^{n} \sin\left(\frac{i\pi x}{l}\right) q_i \tag{4}$$

where $q_i(t)$ are the modes of vibrations of the flexible slider–crank mechanism. To derive the model for the flexible mechanism the Euler–Lagrange equations are used. Let $L = T - U$, where T and U are the kinetic and potential energies of the system, respectively. The equations of motion can be obtained using the following equation:

$$\frac{d}{dt}\left(\frac{\partial L}{\partial \dot{\xi}_i}\right) - \frac{\partial L}{\partial \xi_i} = F_i + \tau_i \tag{5}$$

where F_i are the nonconservative forces, τ_i is the applied torque on the system, and $\vec{\xi}$ is the deflection vector.

$$[\xi_1, \xi_2, ..., \xi_{n+1}] = [\theta, q_1(t), q_2(t), ..., q_n(t)] \tag{6}$$

The kinetic energy of the system is then calculated:

$$T = \frac{1}{2} I_c \dot{\theta}^2 + \frac{1}{2}\rho A \int_0^l \dot{\vec{R}}\,\dot{\vec{R}}\, dx + \frac{1}{2} m_s \dot{X}_B^2 \tag{7}$$

where m_s is the mass of the slider, $\vec{X}_B$ is the velocity of the connecting rod end point, I_c is the moment of inertia of the crank, and ρ, A are the density and cross section of the connecting rod, respectively.

$$\dot{\vec{R}}\,\dot{\vec{R}} = \left(-r\dot{\theta}\sin\theta + \dot{w}\cos\psi + (x+w)\frac{d\cos\psi}{dt}\right)^2 + \left(r\dot{\theta}\cos\theta + \dot{w}\sin\psi + (w-x)\frac{d\sin\psi}{dt}\right)^2 \tag{8}$$

$$\vec{X}_B = \left(-r\dot{\theta}\sin\theta + x\frac{d\cos\psi}{dt}\right)\vec{i} \tag{9}$$

The dependent coordinate ψ is then omitted using the holonomic constraint of the slider–crank mechanism (Eq. (3)). The potential energy of the mechanism is given by

$$U = \frac{1}{2}\int_0^l EI\left(\frac{\partial^2 w}{\partial x^2}\right)^2 dx + m_c g\frac{r}{2}\sin\theta \tag{10}$$

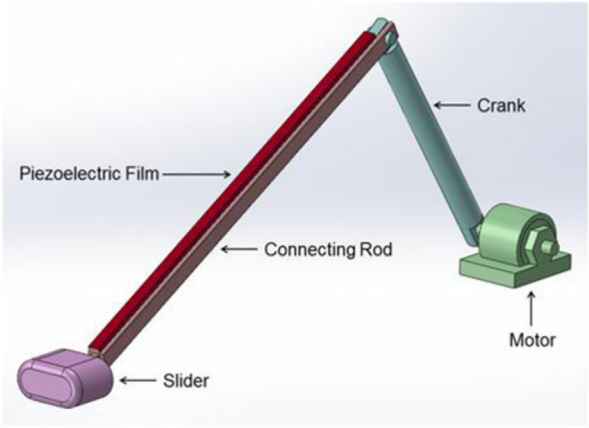

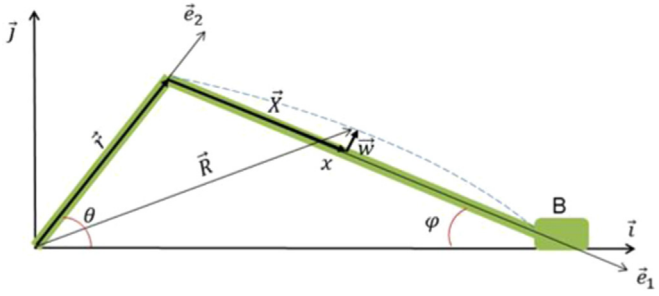

Fig. 1. Slider–crank mechanism.

For a single mode model

$$U = {q_1}^2 \frac{EI}{2}\left(\frac{\pi}{l}\right)^4 \int_0^l \sin^2\frac{\pi x}{l}dx = {q_1}^2 \frac{EI.l}{4}\left(\frac{\pi}{l}\right)^4 + m_c g \frac{r}{2} \sin\theta \tag{11}$$

where EI is the flexural rigidity. The $n+1$ equations of motion of the slider–crank mechanism can be written in the following format.

Now using the potential and kinetic energies defined and introducing the Lagrangian and taking the derivatives the equation of motion of the slider–crank mechanism obtains in this form

$$M\ddot{\xi} + B(\xi,\dot{\xi}) + G(\xi) + F = \tau \tag{12}$$

where M is the mass matrix, which is symmetric and B involves the coriolius and centrifugal terms and G contains the terms of the gravity and the potential energy and F denotes the friction applied to the mechanism and τ is the applied torque at the crank. The equation of the motion is then solved numerically using the ODE function of MATLAB software. Thus the equations are first rewritten in the state-space model.

3. Dynamic behaviour

In this section, effect of the mechanism's parameters on the dynamic response of the system is investigated. A single mode is considered for the connecting rod. Since the connecting rod can be modelled as a pin–pin rod, a single mode is sufficient and accurate enough. The mechanisms' parameters used in the dynamic analysis are listed in Table 1.

Table 1
Mechanism's parameters.

Variable	Definition	Value
R	Crank length	10 cm
L	Connecting rod length	30 cm
Ms	Slider mass	0.5 kg
Mc	Crank mass	2(ρ)(π)hr
EI	Flexibility	0.2
ρ	Material density	7850
H	Radius of the rod	0.02 cm

We have studied effect of the flexibility of the connecting rod, the crank length and the slider mass on the dynamic behaviour of the mechanism.

3.1. Crank length

Small crank angles respect to the connecting rod lengths leads to a smaller amplitude of vibration and a more periodic result.

3.2. Slider mass

As the mass of slider decreases amplitude of vibration of the connecting rod increases and a non-predictable answer obtains for both crank angle of the mechanism and amplitude of vibration.

3.3. Flexibility of the connecting rod

Increasing EI, leads to a more rigid mechanism, and the amplitude of vibration decreases as expected. Phase plane diagram of θ shows a more periodic response.

3.4. Constant angular velocity for crank

Considering a constant angular velocity for the crank eliminates one of the second order differential dynamic equations as the crank angle is known at each time. In this situation amplitude of vibration of the connecting rod is the point of interest.

The frequency response of the amplitude of vibration dependent on the mechanism's parameters at constant crank angular velocity is studied. Amplitude of vibration of connecting rod is plotted respect to the nondimensional crank angular velocity (Figs. 2–4).

$$\Omega = \frac{\omega}{\omega_1}, \quad \omega_1 = \frac{EI\pi^4}{\rho A L^4} \tag{13}$$

where ω_1 is the first natural frequency of a pin–pin beam. When $\Omega = 1$, mechanism undergoes a resonance. Depending on the mechanism's parameters the pick value of the vibration at the resonance frequency differs. The phase plane response at $\Omega = 1$ is plotted in Fig. 5, which indicates an unstable focus and clarifies the instability of the mechanism.

The frequency response of the amplitude of vibration of the connecting rod is depicted in Fig. 6 for a small crank length ($r = 0.003$ m and ms = 0.5 kg). Considering the mechanism's parameters a comparative study is performed on the frequency response of the vibration of the connecting rod (Fig. 7). Pick of

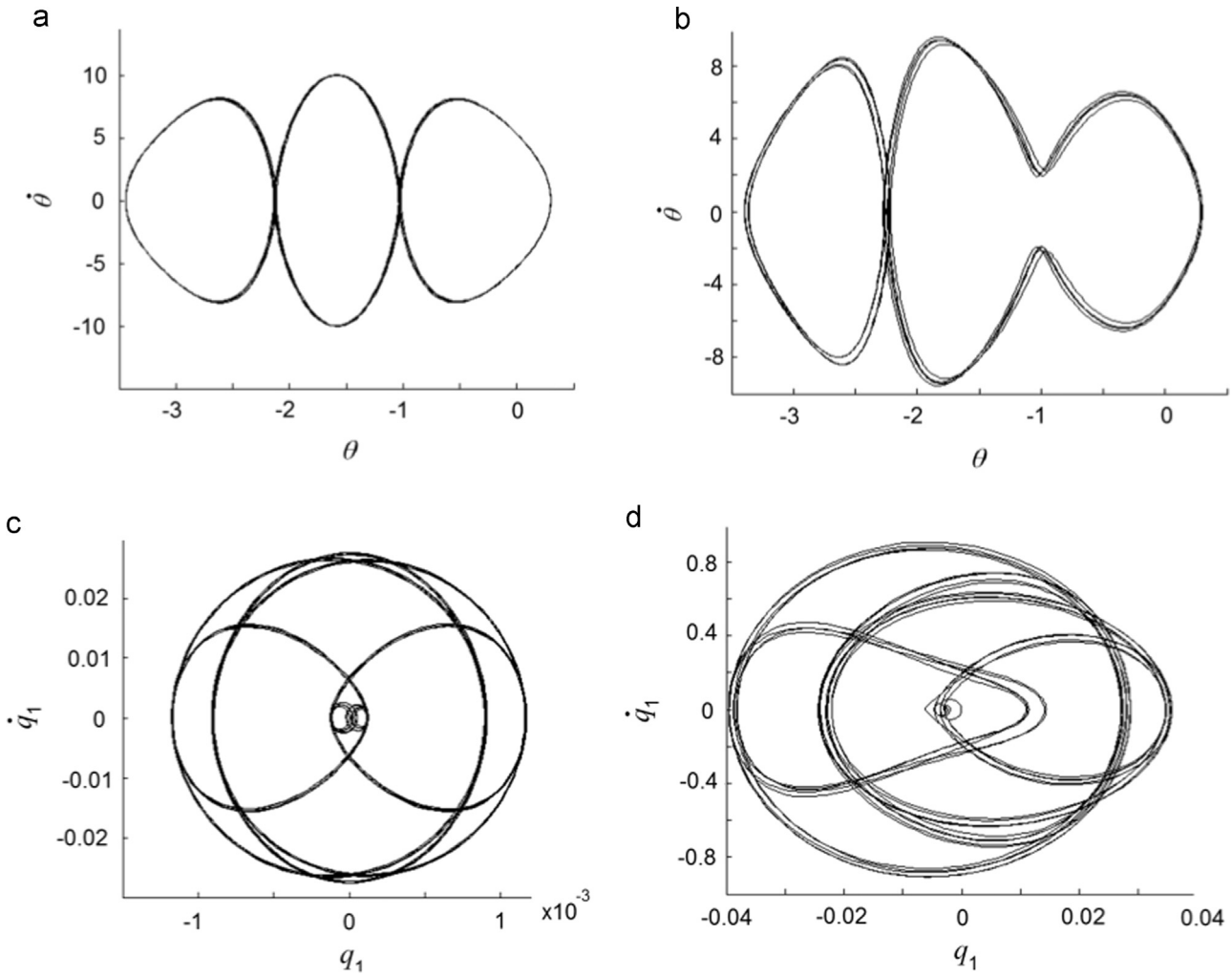

Fig. 2. (a) Phase plane diagram of θ (r=0.003), (b) phase plane diagram of θ (r =0.1), (c) phase plane diagram of q_1 (r=0.003), and (d) phase plane diagram of q_1 (r=0.1).

the resonance amplifies as the crank length increases. Also enough large crank length leads to instability of the mechanism at high frequencies. In other words, increasing the crank length reduces the critical angular velocity.

The phase plane diagram of the amplitude of vibration is then plotted and compared for each Ω.

4. Controller design

In order to design a controller for suppressing the elastodynamic vibrations of the flexible connecting rod, two types of controllers are designed. One is based on the feedback linearization technique and the other is a sliding mode controller, which is a robust control method.

Two kinds of dynamic equations were derived above. In the first one crank angle and its derivatives are considered as states of the dynamic equation and are coupled with the deflection of the flexible connecting rod. For this case a controller based on feedback approach is designed and the elastodynamic vibrations of the flexible connecting rod is suppressed and the crank angle and the angular velocities are tracked a desired sinusoidal path. In the second dynamic equation, a constant angular velocity is considered for the crank and only the deflection of the elastic linkage and its derivative are unknown in the equation. For this case a sliding mode controller is implemented to eliminate and suppress the vibrations of the very flexible connecting rod.

The input control signals are considered to be applied by a motor contrived at the crank ground joint, and two layers of piezoelectric film bonded to the top and bottom surfaces of the connecting rod. The piezoelectric elements exert a distributed moment on the beam, which is proportional to the voltage applied on them. This moment is dependent on several parameters such as the dielectric coefficient, elasticity and thickness of the piezoelement and the connecting rod. The moment value is given by [18,19]

$$M_1 = (E_a w_a t_a t_b)\frac{\gamma}{\gamma+6}\Lambda \ , \ \gamma = \frac{E_b w_b t_b}{E_a w_a t_a} \quad \Lambda = \frac{d_{31}}{t_a}V \tag{14}$$

where E_b, w_b and t_b are the elasticity module, thickness at Y direction and thickness at Z direction of the aluminium beam respectively. E_a, w_a and t_a are the elasticity module and thickness of the piezoactuators. d_{31}, is the dielectric coefficient and V denotes the voltage applied to piezoelement.

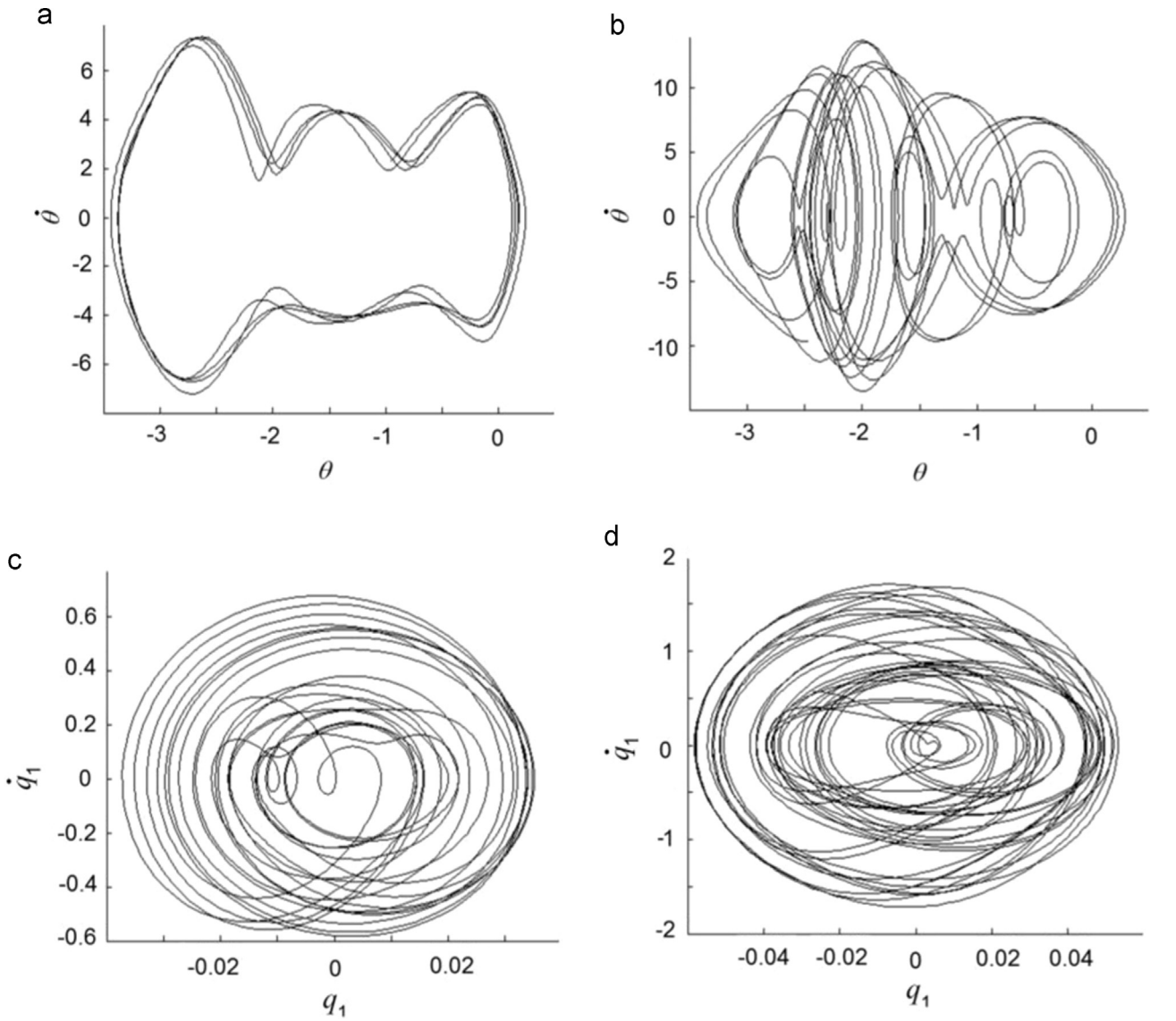

Fig. 3. (a) Phase plane diagram of θ (ms = 5), (b) phase plane diagram of θ (ms = 0.5), (c) phase plane diagram of q_1 (ms = 5), and (d) phase plane diagram of q_1 (ms = 0.5).

Reconsidering the Euler–Lagrange method in deriving the dynamic equations, this moment arises as a moment in the right side of the equation associated with the deflection of the flexible connecting rod that is considered as the control action in this study (Fig. 8).

The open-loop response of the mechanism when a constant input torque is applied to the crank from the motor is depicted in Fig. 9 that indicates the midpoint deflection of the flexible connecting rod. The motor's torque appears only at the first second order differential equation associated with the crank angle. Since the equations of motion of the flexible slider–crank are coupled together, rotation of the crank induces vibration in the connecting rod.

4.1. Controller design via feedback linearization approach

The main idea in this technique is to eliminate nonlinear terms of the dynamic equation of the flexible slider–crank mechanism using state feedback and applying an appropriate input torque to the system.

In this section, it is intended to suppress the vibrations of the elastic linkage besides obtaining a constant angular velocity for the crank. This means that the crank is made to track a desired sinusoidal path. The motor applies one of the torques computed by feedback linearization approach and the other is applied by the piezoelement when the appropriate voltage applied.

$$\tau_1 = \ddot{\theta}_{des} - k_1\dot{\tilde{\theta}} - k_2\tilde{\theta} \tag{15}$$

where θ_{des} is the path that the crank angle is desired to track and $\tilde{\theta}$ is the tracking error.

$$\tau_2 = -k_1^{'}\dot{q}_1 - k_2^{'}q_1 \tag{16}$$

It is desired that q_1 equals to zero, thus $q_{des} \equiv 0, \quad \tilde{q}_1 = q_1$.

k_1, k_2 are the control parameters that guaranty the required behaviour of the closed loop response of the system. Choosing

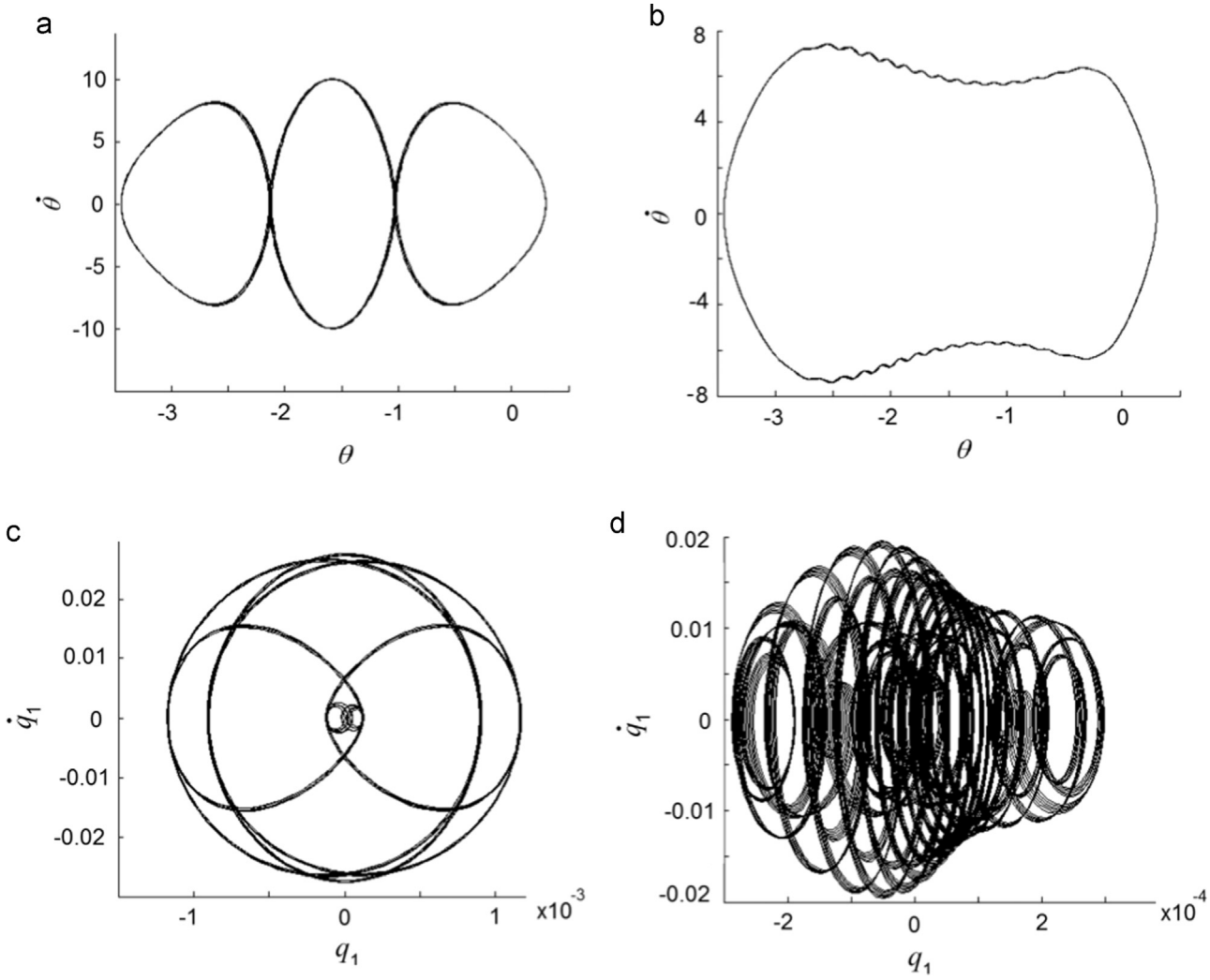

Fig. 4. (a) Phase plane diagram of θ ($EI=0.2$), (b) phase plane diagram of θ ($EI=20$), (c) phase plane diagram of q_1 ($EI=0.2$), and (d) phase plane diagram of q_1 ($EI=20$).

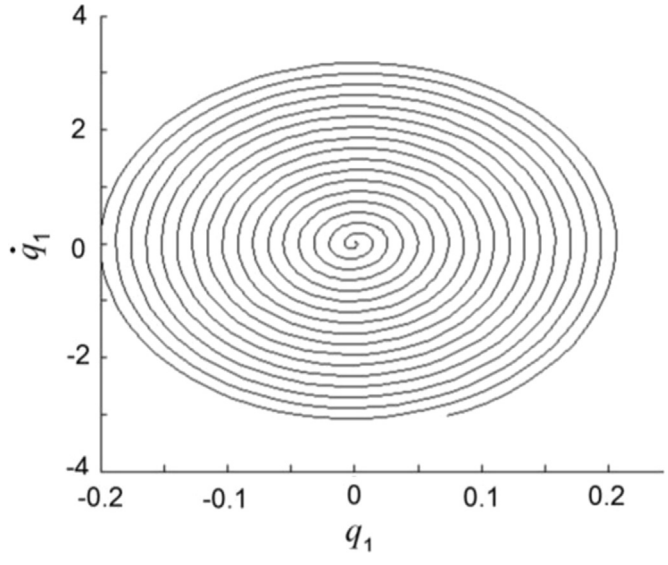

Fig. 5. Phase plane diagram of the amplitude of vibration at $\Omega=1$.

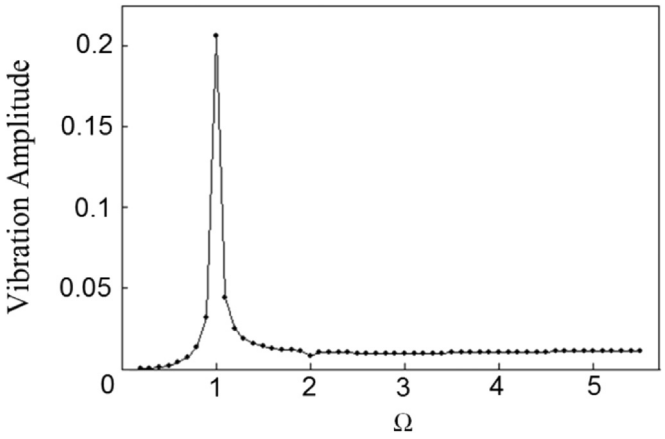

Fig. 6. Frequency response function of the amplitude of vibration.

$k_1=4=2\xi\omega_n$, $k_2=4=\omega_n^2$ a critical damp response obtains. The closed loop responses of the mechanism are plotted in Fig. 10. The controller is turned on after one second.

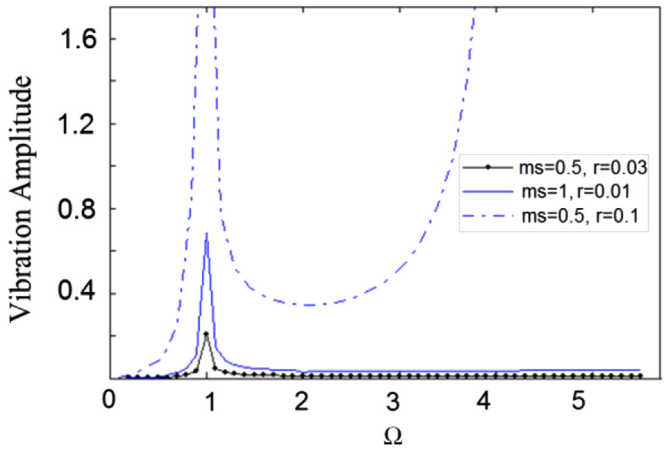

Fig. 7. Dependence of the frequency response on the mechanism's parameters.

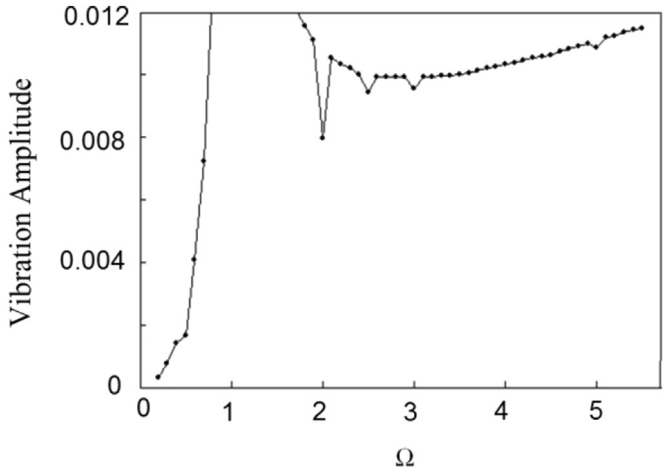

Fig. 8. An undershoot at specific angular velocity.

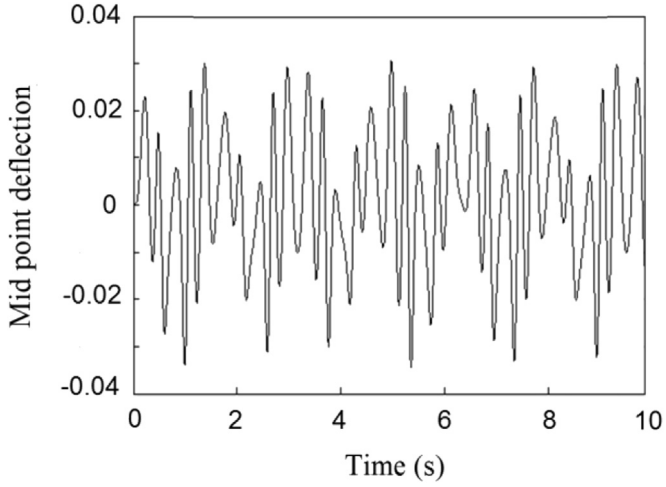

Fig. 9. Open-loop response of the mid point deflection of the flexible connecting rod.

It is observed that the designed controller suppresses the elastodynamic vibrations of the flexible connecting rod efficiently and the crank angle and the angular velocity track the desired sinusoidal path as required. The phase plane diagram of the crank angle also confirms the periodic desired path for the crank.

4.2. Controller design via sliding mode approach

The sliding mode control is a variable structure and also a robust control method. A notational simplification is introduced in this method, which allows nth order problems to be replaced by equivalent 1st order problems that are much easily controlled.

A time varying surface $s(t)$ is defined by the scalar equation $s(x,;t)=0$, where

$$s(x;t)=\dot{\tilde{q}}_1+\lambda\tilde{q}_1=0 \tag{17}$$

where $\tilde{q}_1$ is the tracking error. In suppression of the elastodynamic vibrations of a slider–crank mechanism, the desired q_1 equals to zero.

The problem of tracking $\tilde{q}_1\to 0$ is equivalent to approaching to the sliding surface and remaining on it. Indeed $s\equiv 0$ represents a linear differential equation whose unique equilibrium point is $\tilde{q}\equiv 0$.

A positive definite Lyapanov function is defined as

$$V(s)=\frac{1}{2}s^2 \tag{18}$$

Derivative of $V(s)$ guaranties the stability and tracking of the system.

$$\dot{V}(s)=\frac{1}{2}\frac{d}{dt}s^2=s.\dot{s} \tag{19}$$

The input control signal is then designed to satisfy the below condition

$$\dot{V}(s)=\frac{1}{2}\frac{d}{dt}s^2=s.\dot{s}\le-\eta|s| \tag{20}$$

The above inequality states that the squared distance to the surface as measured by s^2 decreases along all system trajectories. Thus, it constraints trajectories to point toward the sliding surface $s(t)$.

A control law based on Eq. (20) is implemented on the dynamic equation of the flexible connecting rod, while a constant angular velocity is assumed.

$$M\ddot{q}_1+B(q_1,\dot{q}_1)=\tau_2\Rightarrow\ddot{q}_1=F(q_1,\dot{q}_1)+u \tag{21}$$

where $F=\frac{-B}{M}$, *and* $\tau_2=M.u$

$$s(x;t)=\tilde{q}^1+\lambda\tilde{q}_1=0 \tag{22}$$

$$\dot{V}(s)=\frac{1}{2}\frac{d}{dt}s^2=s.\dot{s}\le-\eta|s|$$
$$\Rightarrow\begin{cases}s<0, & u=\eta-F-\lambda\dot{q}_1\\ s>0, & u=-\eta-F-\lambda\dot{q}_1\end{cases} \tag{23}$$

Eq. (23) implies a dissentious control law for the system. The closed loop responses indicated that the trajectories of the system approaches to the sliding surface and tries to stay on it. Since the implementation of the associated control switching is not instantaneous, chattering occurs, which is undesirable in

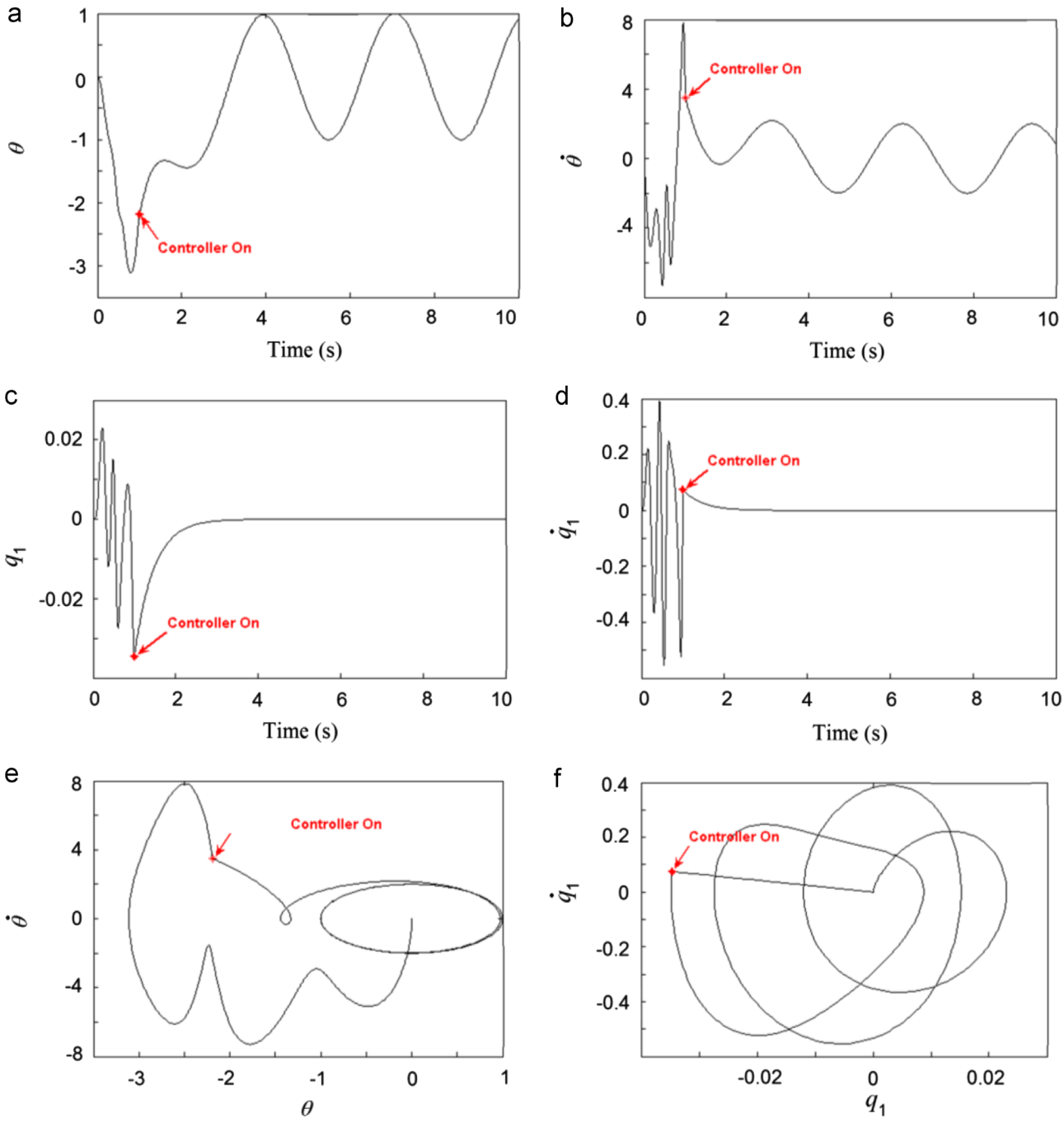

Fig. 10. (a) Closed-loop response of the crank angle (via feedback linearization approach), (b) closed-loop response of $\dot{\theta}$ (via feedback linearization approach), (c) closed-loop response of mid point deflection (via feedback linearization approach), (d) closed-loop response of $\dot{q}_1$ (via Feedback Linearization approach), (e) phase plane diagram of θ, (f) phase plane diagram of q_1.

practice, since it involves high control activity and failure of the piezoactuators (Fig. 11).

A new control law based on the Filippov's method for construction of the equivalent dynamics is presented here to eliminate the chattering. After reaching the trajectories to the sliding surface an equivalent control signal u_{eq} which can be interpreted as a continuous control law is applied to the system. The closed loop responses of the system based on the sliding mode approach and considering the Filippov's method are then plotted in Figs. 12 and 13. As indicated in the figures chattering is eliminated. In this system λ is chosen to be 3 and $\eta = 0.5$. The angular velocity for the crank is $\omega = 0.4\omega_1$.

5. Conclusion

Dynamic behaviour of a slider–crank mechanism with a flexible connecting rod is investigated. The equations of motion of the mechanism are derived using Euler–Lagrange method and the mode summation technique. The dynamic response of the system depends on the mechanisms'

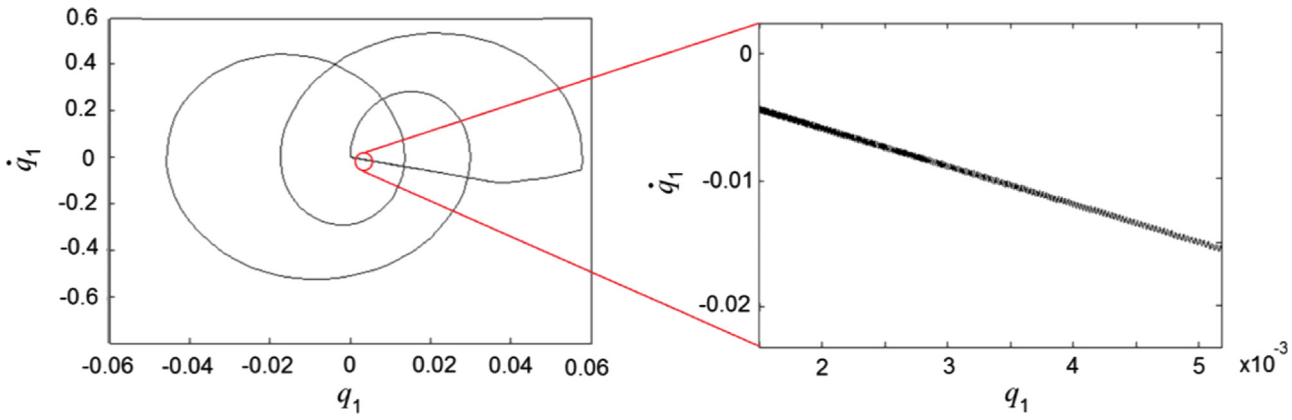

Fig. 11. Phase Plane diagram of the elastodynamic vibrations.

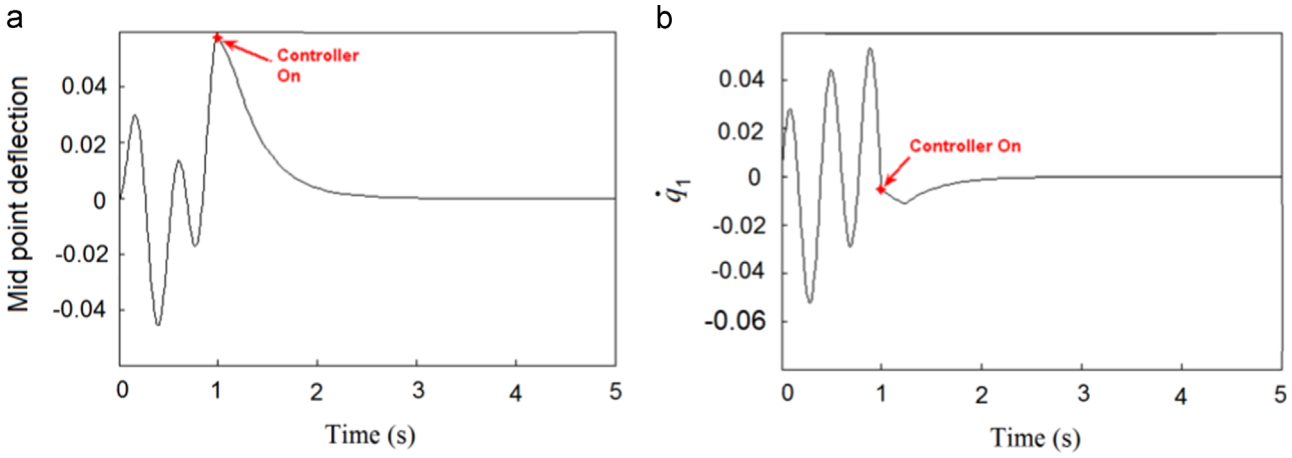

Fig. 12. (a) Closed loop response of q_1, (b) closed-loop response of $\dot{q}_1$.

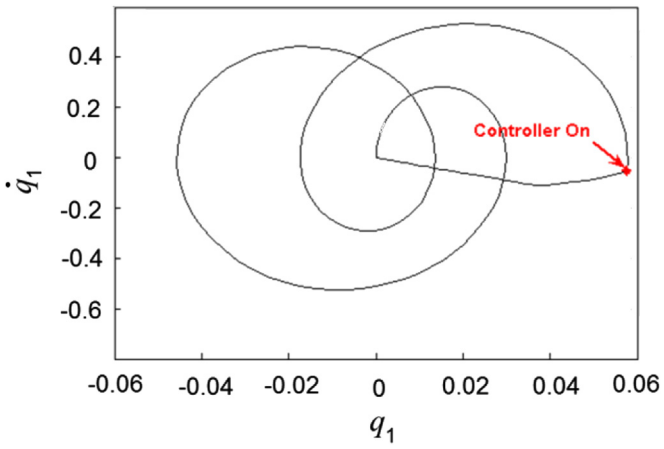

Fig. 13. Phase plane diagram of q_1 (chatter is eliminated).

parameters. We have investigated the effect of crank length, flexibility of the connecting rod and the slider mass on the dynamic behaviour of the system. Increasing the crank length leads to higher amplitude of vibration and in an unpredictable motion of the mechanism. Decreasing the slider mass and increasing the flexibility of the connecting rod result in the same conclusions. Noticing the frequency response function, increasing the crank length increases pick value at the resonance and also decreases the critical velocity, which destabilizes the mechanism. Two control schemes are employed for elastodynamic vibration suppression of the flexible connecting rod. First scheme is based on feedback linearization and the second one is a sliding mode controller. Performance of the sliding mode controller is then improved by considering the Filippov's method and the chattering is eliminated. The control actions are applied by an electric motor at the crank ground joint, and two layers of piezoelectric film bonded to the top and bottom surfaces of the connecting rod.

References

[1] Khemili I, Romdhane L. Dynamic analysis of a flexible slider–crank mechanism with clearance. *Eur. J. Mech – A/Solids* 2008;**27**:882–98.
[2] Hsieh SR, Shaw SW. The dynamic stability of and nonlinear resonance of a flexible connecting rod: single mode model. *J. Sound Vib.* 1994;**170**: 25–49.
[3] Jen-San C, Chu-Hsian C. Effect of crank length on the dynamic behaviour of a flexible connecting rod. *ASME J. Vib. Acoust.* 2001;**123**: 318–23.
[4] Zheng E, Zhou X. Modeling and simulation of flexible slider–crank mechanism with clearance for a closed high speed press system. *Mech. Mach. Theory* 2014;**74**:10–30.

[5] Reis VL, Daniel GB, Cavalca KL. Dynamic analysis of a lubricated planar slider–crank mechanism considering friction and Hertz contact effects. *Mech. Mach. Theory* 2014;**74**:257–73.
[6] Muvengei O, Kihiu J, Ikua B. Numerical study of parametric effects on the dynamic response of planar multi-body systems with differently located frictionless revolute clearance joints. *Mech. Mach. Theory* 2012;**53**:30–49.
[7] Zhang X, Mills JK, Cleghorn WL. Experimental implementation on vibration mode control of a moving 3-PRR flexible parallel manipulator with multiple PZT transducers. *J. Vib. Control* 2010.
[8] Kao CC, Chuang CW, Fung RF. The self-tuning PID control in a slider–crank mechanism system by applying particle swarm optimization approach. *Mechatronics* 2006;**16**(8)513–22.
[9] Zhang X, Shao C, Li S, Xu D, Erdman AG. Robust H∞ vibration control for flexible linkage mechanism systems with piezoelectric sensors and actuators. *J. Sound Vib.* 2001;**243**(1)145–55.
[10] Mansour AK. Control of the elastodynamic vibrations of a flexible slider–crank mechanism using -synthesis. *Mechatronics* 2000;**10**:649–68.
[11] Karkoub M, Yigit AS. Vibration control of a four-bar mechanism with a very flexible coupler. *J. Sound Vib.* 1999;**222**:171–89.
[12] Sannah M, Smaili A. Active control of elastodynamic vibrations of a four-bar mechanism system with smart coupler link using optimal multivariable control: experimental implementation. *Trans. ASME J. Mech. Des* 1998;**120**:316–26.
[13] Pirbodaghi T, Fesanghary M, Ahmadian MT. Non-linear vibration analysis of laminated composite plates resting on non-linear elastic foundations. *J. Frankl. Inst.* 2011;**348**:353–68.
[14] Pirbodaghi T, Ahmadian MT, Fesanghary M. On the homotopy analysis method for non-linear vibration of beams. *Mech. Res. Commun.* 2009;**36**:143–8.
[15] Steen K. Complex modes and frequencies in damped structural vibrations. *J. Sound Vib.* 2004;**270**:981–96.
[16] Pirbodaghi T, Hoseini S. Nonlinear free vibration of a symmetrically conservative two-mass system with cubic nonlinearity. *J. Comput. Nonlinear Dyn.* 2009;**5**(1)011006.
[17] Hoseini SH, Pirbodaghi T, Ahmadian MT, Farrahi GH. On the large amplitude free vibrations of tapered beams: an analytical approach. *Mech. Res. Commun.* 2009;**36**(8)892–7.
[18] Chopra I. Review of state of art of smart structures and integrated systems. *AIAA J.* 2002;**40**:2145–87.
[19] Cameron B, Larry LH, Spencer PM, Mark SE. Dynamic modelling of compliant constant-force compression mechanisms. *Mech. Mach. Theory* 2003;**38**:1469–87.